*Plant Physiology*, April 2000, Vol. 122, pp. 1323–1333, www.plantphysiol.org © 2000 American Society of Plant Physiologists

# Programmed Cell Death during Pollination-Induced Petal Senescence in Petunia[1]

**Yan Xu and Maureen R. Hanson***

Department of Molecular Biology and Genetics, Cornell University, Ithaca, New York 14853

**Petal senescence, one type of programmed cell death (PCD) in plants, is a genetically controlled sequence of events comprising its final developmental stage. We characterized the pollination-induced petal senescence process in *Petunia inflata* using a number of cell performance markers, including fresh/dry weight, protein amount, RNA amount, RNase activity, and cellular membrane leakage. Membrane disruption and DNA fragmentation with preferential oligonucleosomal cleavage, events characteristic of PCD, were found to be present in the advanced stage of petal senescence, indicating that plant and animal cell death phenomena share one of the molecular events in the execution phase. As in apoptosis in animals, both single-stranded DNase and double-stranded DNase activities are induced during petal cell death and are enhanced by $Ca^{2+}$. In contrast, the release of cytochrome *c* from mitochondria, one commitment step in signaling of apoptosis in animal cells, was found to be dispensable in petal cell death. Some components of the signal transduction pathway for PCD in plants are likely to differ from those in animal cells.**

Programmed cell death (PCD) is a genetically defined process associated with common morphological and biochemical changes (Steller, 1995). It is well established that PCD is an intrinsic part of the life cycle of all multicellular organisms studied so far, including both animals and plants (Ellis et al., 1991; Greenberg, 1996; Pennell and Lamb, 1997; Green, 1998). This default cell-suicide process can be initiated by a variety of stimuli, including developmental signals and environmental cues (Vaux and Strasser, 1996; Wertz and Hanley, 1996). PCD is critical for normal development, maintenance of tissue homeostasis, and the defense response (White, 1996; Mittler, 1998). One important function in plant PCD is to remobilize as much nutrition as possible to benefit the plant on the whole level (Smart, 1994).

The most widely studied PCD is animal cell apoptosis, which is characterized by a distinct set of morphological and biochemical features. The common morphological changes associated with apoptosis include cell shrinkage, cytoplasmic membrane blebbing, nuclei lobing, DNA fragmentation, and disassembly into apoptotic bodies rapidly engulfed by phagocytes or neighboring cells in the absence of adverse inflammatory reaction (Steller, 1995). At the molecular level, extensive studies have revealed many events during apoptosis, and the basic signaling framework has been established (for review, see Osborne and Schwartz, 1994; Steller, 1995; Vaux and Strasser, 1996; Jacobson et al., 1997; Wilson, 1998; Vaux and Korsmeyer, 1999). Apoptotic stimuli deactivate the suppression of PCD by anti-apoptotic molecules that unleash the protease activities of a subset of Cys proteases, the caspases. The action of caspases on their downstream substrates causes apoptotic morphological changes and leads to cell death.

In apoptosis, the emergent view is that the molecular events occurring in the mitochondria appear to be a "point of no return" for the cell, an ultimate commitment to cell death (Bossy et al., 1998; Cai et al., 1998; Green and Kroemer, 1998; Green and Reed, 1998). Many members of the Bcl-2 family, the most important regulators in apoptosis, reside in the mitochondrial outer membrane (Reed, 1997a). The interactions among Bcl-2 family members are believed to trigger the changes associated with mitochondria (Mahajan et al., 1998; Schendel et al., 1998; Finucane et al., 1999). An early event in apoptosis, the release of cytochrome *c* (Cyt *c*)from the intermembrane space of mitochondria to the cytosol, has been considered a prerequisite for apoptosis (Reed, 1997b; Yang et al., 1997). Once Cyt *c* is released, the cell will die, either by a rapid apoptotic mechanism involving caspase activation or by a slower necrotic process due to the collapse of electron transport, the generation of reactive oxygen species, and a decrease in ATP production (Green and Reed, 1998). In addition, collapse of mitochondrial inner transmembrane potential causes the release of other factors, including an apoptosis-inducing factor (Susin et al., 1999b) and procaspase-2 and -9 (Susin et al., 1999a), which are also important molecules for the execution of apoptosis.

PCD is an integral part of normal plant development, including embryogenesis, floral organ abortion, root cap sloughing, senescence, and the development of gametophytes and vascular tissue (for review, see Jones and Dangl, 1996; Pennell and Lamb, 1997; Mittler, 1998). During these developmental processes, cell death may occur at the level of individual cells and can involve a single tissue layer or an entire organ. DNA fragmentation is the most widely evaluated criterion for PCD. Due to the preferential digestion of nDNA at internucleosomal sites, a DNA ladder can be visualized as 160-bp multiples on the gel. Such a DNA ladder has been observed in plant PCD, including

[1] This research was supported by the U.S. Department of Agriculture Hatch Program and the Energy Biosciences Program of the U.S. Department of Energy (grant no. FG02–89ER14030 to M.R.H.), and by a fellowship from the Cornell National Science Foundation/Department of Energy/U.S. Department of Agriculture Plant Science Center (to Y.X.).

* Corresponding author; e-mail mrh5@cornell.edu; fax 607–255–6249.

that in aleurone layers during seed germination (Wang et al., 1998), anther development (Wang et al., 1999), old Arabidopsis cell cultures (Callard et al., 1996), senescing pea petal and ovary (Orzaez and Granell, 1997a, 1997b), leaf senescence (Yen and Yang, 1998), stress treatment (Katsuhara and Kawasaki, 1996; Katsuhara, 1997; Koukalova et al., 1997; Danon and Gallois, 1998), and in response to pathogens or toxins (Ryerson and Heath, 1996; Wang et al., 1996a, 1996b; Navarre and Wolpert, 1999). Other apoptotic features are selectively present in different types of plant PCD studied so far, including cell shrinkage, chromatin condensation, nuclei lobing, and the formation of apoptotic bodies (Mittler and Lam, 1995; Callard et al., 1996; Levine et al., 1996; Fukuda, 1997; Mittler et al., 1997; Groover and Jones, 1999).

Two recent studies explored the involvement of Cyt *c* in plant cell death. With the addition of Cyt *c*, the cytosol of carrot cells induced mouse liver nuclei to undergo a typical apoptosis, which could be inhibited by caspase inhibitors (Yun et al., 1999). D-Man treatment not only promoted DNA laddering in maize cell suspensions, but also induced Cyt *c* release into the cytosol (Stein and Hansen, 1999). However, the timing of the Cyt *c* release was correlated with the degree of DNA laddering, in striking contrast to the early release in animal apoptosis, in which there are no nuclear morphological changes (Reed, 1997b). The reported Cyt *c* relocation at a late stage of cell death might have been a secondary effect of loss of mitochondrial integrity.

Petal senescence is an active process requiring new gene expression at both the transcriptional and the translational levels (Lawton et al., 1990; Nooden et al., 1997). Treatments with actinomycin D or cycloheximide generally retard petal senescence (Wulster et al., 1982; Lay-Yee et al., 1992; Jones et al., 1994). Several genes highly up-regulated in senescing petals have been isolated, including 1-aminocyclopropane-1-carboxylic acid (ACC) synthase and ACC oxidase (Tang and Woodson, 1996; Clark et al., 1997; Jones and Woodson, 1999), a thiol protease (Jones et al., 1995), a glutathione *S*-transferase (Meyer et al., 1991), an enzyme involved in phosphonate biosynthesis (Wang et al., 1993), wall-based enzymes (Panavas et al., 1998a), and some genes of unknown function (Lawton et al., 1989; Raghothama et al., 1991; Jiang et al., 1994; Do and Huang, 1997).

It is well known that compatible pollination triggers a series of post-pollination developmental events, including ovary growth (Zhang and O'Neill, 1993), pigmentation changes (Whitehead et al., 1984), and petal senescence (Reid and Wu, 1992; Stead, 1992). The biochemical changes associated with petal senescence, including an increase in hydrolytic enzymes, degradation of macromolecules, and an increase in respiratory activity, constitute a predictable programmed process (Reid and Wu, 1992).

Floral senescence in *Petunia* species has previously been studied primarily with regard to the role of ethylene. As in other ethylene-sensitive flowers, autocatalytic ethylene production is characteristic of *Petunia* petal senescence with or without pollination (Hoekstra and Weges, 1986; Singh et al., 1992). Exogenous ethylene accelerated petal color changes and wilting of *Petunia hybrida* (Whitehead et al., 1984), while inhibitors of ethylene biosynthesis and action retarded senescence (Hoekstra and Weges, 1986; Serek et al., 1995). In the self-incompatible species *Petunia inflata*, Singh et al. (1992) found that both self-incompatible and self-compatible pollination resulted in production of ethylene about 3 h after pollination, but then floral ethylene production declined to a low level until 18 h, when another increase in ethylene began to occur in compatibly-pollinated flowers but not in flowers receiving incompatible pollen. Because petal senescence can be triggered reproducibly by compatible pollination in *P. inflata*, we chose this species as a model system for investigating PCD during pollination-induced petal senescence (PIPS).

Despite the long-term interest in floral degeneration, comprehensive physiological studies have been limited to petal senescence in carnation and daylily. In this study, we characterized *Petunia* PIPS by evaluating a number of parameters typically measured during floral degeneration, such as fresh/dry weight, water content, protein degradation, and membrane integrity. Furthermore, we examined DNase activity, DNA fragmentation, and Cyt *c* compartmentation, factors known to change during certain types of PCD.

## MATERIALS AND METHODS

### Plant Growth and Pollination

Two different *Petunia inflata* populations bearing different S alleles can be used to pollinate each other. A line termed *P. inflata-1* was derived from seed originally received from Ken Sink (Michigan State, East Lansing, MI). The other population, termed P-S-14, was provided by D. Maizonnier (Dijon, France), who obtained it from a South American source. Plants were grown at 74°F under 16 h of daylight and 8 h of darkness. The compatibility of P-S-14 pollen on *P. inflata-1* was confirmed by seed production, while self-pollination of *P. inflata-1* flowers did not result in seed set. Pollen from P-S-14 was used to pollinate *P. inflata-1* on the day of flower opening. At pollination, the five stamens were removed from *P. inflata-1* flowers to reveal the stigma and to avoid incompatible pollination.

### Fresh Weight and Dry Weight Determination

Eight corollas collected at 0, 12, 24, 36, and 48 h after compatible pollination (HACP) were weighed (fresh weight) and then baked at 80°C for about 10 h until completely dry (dry weight). The average fresh weight per corolla was used in expressing the RNA/protein amount on a corolla basis.

### RNA Isolation and Quantitation

Petal corollas were frozen in liquid $N_2$ directly after collection and kept at −80°C until use. Total RNA was extracted by TRIZOL reagent according to the manufacturer's instruction (BRL, Gaithersburg, MD). RNA amount was determined by $OD_{260}$, and the concentration was confirmed by electrophoresis on a denaturing gel containing formaldehyde (Maniatis et al., 1989).

### Protein Extraction and Quantitation

For protein extraction, frozen tissues were ground in liquid $N_2$. After adding extraction buffer (50 mM Tris, pH7.6, 2 mM EDTA, 2% [w/v] SDS, 2 mM dithiothreitol (DTT), 14 mM $\beta$–mercaptoethanol, and 1 tablet of EDTA-free protease inhibitor [BRL] for each 30 mL of buffer), samples were boiled at 100°C for 3 min and centrifuged at 10,000*g* for 3 min. The supernatant was used for protein quantitation by a modified Lowry method (Larson et al., 1986). Protein concentration was further confirmed by SDS-PAGE.

### Membrane Leakage

Measurement of ion leakage from corollas was performed essentially as described in Panavas et al. (1998b) with some modifications. Eight corollas were cut off at the junction point with the corolla tube at 0, 12, 24, 36, and 48 HACP, incubated in 50 mL of double distilled water for 1 h under gentle shaking. This solution was tested for sample conductivity. Then the corollas were boiled in 50 mL of double-distilled water for 5 min, and this solution was measured to obtain the subtotal conductivity. Membrane leakage is represented by the relative conductivity, which was calculated as sample conductivity divided by total conductivity (the sum of sample conductivity and subtotal conductivity). Conductivity of the solutions was measured with a conductivity meter (model CDM80, Radiometer, Copenhagen).

### Activity Gel Assays

The detection of DNase and RNase activities was based on the methods of Blank and McKeon (1991) and Panavas et al. (1998b) with the following modifications. The resolving gel contained 100 $\mu$g/mL bovine serum albumin (BSA) and 40 $\mu$g/mL *Petunia* total leaf RNA for RNase activity or 15 $\mu$g/mL salmon DNA for DNase activity (for single-stranded DNase activity, salmon DNA was boiled for 3 min before use). Equal amounts of total protein from 0, 12, 24, 36, or 48 HACP were boiled for 1 min in 1× SDS sample buffer (50 mM Tris, pH 6.8, 1% [w/v] SDS, 5% [w/v] glycerol, 100 mM DTT, and 0.01% [w/v] bromphenol blue) before loading on 10% SDS-PAGE gels. After electrophoresis, the resolving gel was renatured in renaturation buffer A (0.1 M Tris, pH 7.4, 1% [v/v] Triton X-100, and 5 mM $CaCl_2$) at 37°C with periodic shaking. The buffer was changed every 30 min until the bromphenol blue dye disappeared. To study the effect of bivalent ions on DNase and RNase activities, renaturation buffer B (0.1 M Tris, pH 7.4, 1% [v/v] Triton X-100, and 20 mM NaCl) was used instead. After a brief rinse in 0.1 M Tris, pH 7.2, tests for enzymatic activity were carried out at 37°C. To detect DNase activity, the gel was incubated overnight in basic buffer (50 mM Tris, pH 7.0, 20 $\mu$M $CaCl_2$, 10 $\mu$M $MgCl_2$, and 20 mM NaCl) or basic buffer plus additional chemicals as indicated in the figure legends. The same buffers were used for RNase activity analysis with a 2-h incubation time. Nucleic acids in the gel were visualized by staining with 0.1 M Tris, pH 7.2, containing 0.5 $\mu$g/mL ethidium bromide for 1 h. Upon UV illumination, DNase or RNase activity was visualized as a clear band in a stained field.

### Cellular Fractionation and Immunoblotting

Two grams of corolla tissue (about 20–30 corollas) from 0, 24, and 30 HACP was ground in grinding buffer (0.4 M mannitol, 1 mM EGTA, 20 mM $\beta$–mercaptoethanol, 50 mM Tricine, and 0.1% [w/v] BSA, pH 7.8) for 40 s at 4°C. Extracts were filtered through four layers of cheesecloth and one layer of Miracloth (Calbiochem, La Jolla, CA), and the retained liquid was squeezed out. The filtrate (crude corolla extract) was centrifuged at 1,500*g* for 5 min at 4°C. The pellet, containing mainly nuclei and chloroplasts, was resuspended in grinding buffer. The supernatant (extract devoid of nuclei and chloroplasts) was centrifuged at 16,000*g* for 15 min at 4°C. Following this second centrifugation, the supernatant thus obtained was taken to represent the cytosol fraction, and the pellet was resuspended in grinding buffer to represent the mitochondria fraction. Protein concentration was measured by Bradford reagent (Bio-Rad Laboratories, Hercules, CA) using BSA as a standard. Fifty micrograms of total protein was separated on 12% SDS-PAGE gels. Cyt *c* from bovine heart (Sigma-Aldrich, St. Louis) was used as a positive control. A monoclonal anti- Cyt *c* antibody from Pharmingen (San Diego) was used for immunoblot detection.

### DNA Fragmentation Analysis

Genomic DNA from petals of pollinated flowers at 0, 12, 24, or 36 HACP or unpollinated flowers 6 d after opening was isolated according to a modified cetyl-trimethyl-ammonium bromide (CTAB) method (Fulton et al., 1995). Equal amounts of genomic DNA was separated on a 2% (w/v) agarose gel and transferred to Hybond $N^+$ membrane (Amersham, Piscataway, NJ). Probe labeling was with a random labeling kit (DECAprime II, Ambion, Austin, TX). After overnight hybridization, filters were washed twice with 0.2× SSC/0.1% (w/v) SDS at 65°C.

## RESULTS

### Effects of Pollination on Petal Senescence

Singh et al. (1992) have shown that compatible pollination induced signs of flower wilting as early as 36 HACP in detached *P. inflata* flowers. Since flowers on plants showed different wilting time courses than detached flowers (Reid and Wu, 1992), the effect of pollination in planta was studied. Pollination was carried out by depositing either compatible pollen from P-S-14 or self-pollen on the stigmas of emasculated flowers of *P. inflata-1* on the day of flower opening. Wilting was observed clearly at 36 HACP (Fig. 1), which is consistent with a previous report (Singh et al., 1992). In contrast to this rapid effect of compatible pollination, the degree of wilting at 36 HACP shown in Figure 1 was not observed until about 4 d after incompatible pollination or around 6 d after flower opening (data not

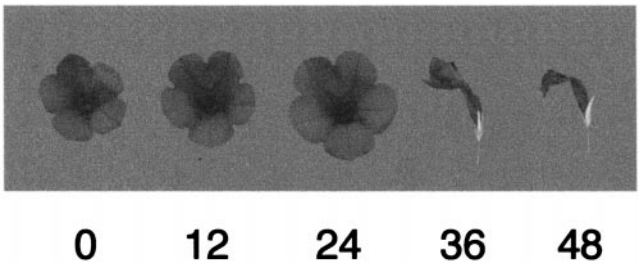


**Figure 1.** Effect of compatible pollination on petal senescence in *P. inflata*. Flowers of *P. inflata-1* were pollinated by pollen from *P. inflata* P-S-14 on the day of flower opening. 0, 12, 24, 36, and 48, HACP.

shown). To determine whether pollination-induced wilting can be caused by unrelated pollen, pollen from tobacco (*Nicotiana tabacum*) was applied to the stigma of *P. inflata* plants. However, this pollination did not affect the rate of petal senescence (data not shown), suggesting that the accelerated wilting response observed depends on the specific recognition of compatible pollen.

There are two major visual changes during petal senescence in *P. inflata*: the change of petal color and the collapse of petal shape. During senescence of either intact flowers (data not shown) or detached flowers (Singh et al., 1992) that were not compatibly pollinated, a gradual alteration in color occurs over about 5 d before severe degeneration occurs. In detached, compatibly-pollinated *P. inflata* flowers, Singh et al., (1992) observed color changes before obvious wilting. In contrast, we observed that compatible pollination results in floral collapse before the color change when the flowers were not removed from the plant (data not shown). Our results indicated that compatible pollination affects the timing of the morphological versus pigmentation changes on intact flowers.

### Biochemical Changes in PIPS

The degree of senescence is generally exemplified by changes in a set of physiological parameters, including fresh/dry weight, RNA amount, protein amount, and cellular membrane leakage (Smart, 1994). The profiles of these changes, especially whether different profiles were correlated with each other in the whole process, were examined in our system. Each parameter was analyzed at three levels: per corolla, per unit fresh weight, and per unit dry weight, each providing a different basis for comparison. To minimize the influence of random environmental fluctuations or biological variations, eight corollas were pooled at each time point during the same pollination experiment, and at least six independent pollination experiments were analyzed for each parameter.

As shown in Figure 2A, both fresh weight and dry weight increased until 24 HACP and dropped dramatically at 36 HACP. Water content, represented by the ratio of dry weight to fresh weight, was constant up to 24 HACP and then started to increase. This result is consistent with the traditional concept that the loss of water content in petal tissues contributes to wilting symptoms (Nooden et al., 1997). In contrast to the increase in corolla size until 24 HACP (Fig. 1), which was also reflected by the increase in the fresh/dry weight (Fig. 2A), the amounts of RNA (Fig. 2B) and protein (Fig. 2C) decreased continuously after pollination. These results suggest that compatible pollination triggers molecular changes at a very early stage, despite a healthy appearance of the petal and the increase in the physical size of the petal.

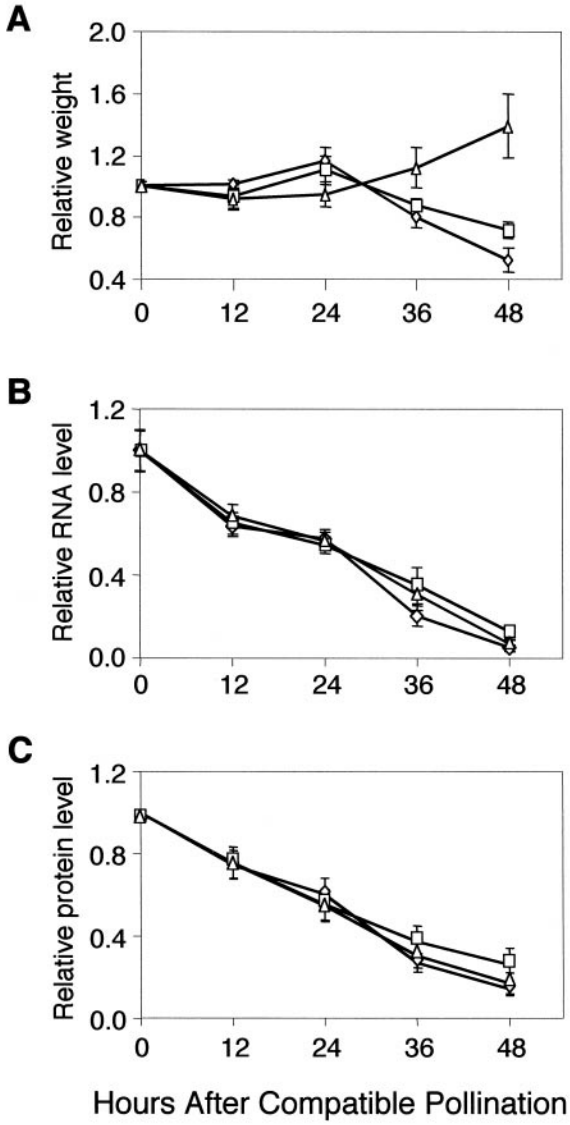


**Figure 2.** Effects of compatible pollination on weight (A), protein (B), and RNA (C). Eight corollas were taken at each time point for different measurements. The average result of six independent pollination experiments was presented. For the data per corolla, data were recalculated based on the average fresh weight at each time point in order to make different parameters more comparable. Data are shown as a ratio of the parameter at the time point versus the parameter at time of flower opening. Error bars indicate the SD. 0, 12, 24, 36, and 48, HACP. A, ◇, Fresh weight/corolla; □, dry weight/corolla; △, dry weight/fresh weight. B, ◇, RNA/corolla; □, RNA/unit fresh weight; △, RNA/unit dry weight. C, ◇, Protein/corolla; □, protein/unit fresh weight; △, protein/unit dry weight.

Plant cell death is also associated with an increase in cellular membrane leakage (Borochov et al., 1997; Pontier et al., 1998), which can be measured by ion leakage. In PIPS, membrane leakage remains constant until 24 HACP, and increases dramatically at 36 HACP (Fig. 3), correlating with the visual wilting symptoms (Fig. 1) but lagging behind RNA/protein changes (Fig. 2, B and C). This result suggests that the cellular membrane is intact at the early stage of PIPS.

### Both Constitutive and Novel RNase Activities Contribute to RNA Degradation

To find out whether the degradation of RNA is due to stage-specific RNases or to the up-regulation of certain constitutive activities, RNase activity in total protein extracts from corolla tissue was analyzed in activity gels. The experimental conditions were optimized for the detection of the maximum number of RNase bands. As shown in Figure 4A, two major RNase bands (R1 and R2) were present in both open petals and senescing petals at 36 HACP. Two additional RNase bands (R3 and R4) appeared in senescing petals at 36 HACP, but not in open petals (Fig. 4A), suggesting that there are novel RNase activities in PIPS. Several RNase bands between R1 and R2 showed weak activity, which were likely to result from low abundance or unfavorable enzymatic reaction conditions.

To examine how the constitutive and novel RNase activities were regulated during PIPS, RNase activities were monitored over time. Figure 4B reveals that R1 and R2 were present in both healthy and wilted corolla, and the total amount of constitutive RNase activity increased after 12 HACP. Novel RNase activities, on the other hand, appeared at 12 HACP and increased up to 48 HACP (Fig. 4B). Although RNA amounts decreased continuously after compatible pollination (Fig. 2C), the new RNase activities did not increase substantially until after 24 HACP (Fig. 4B).

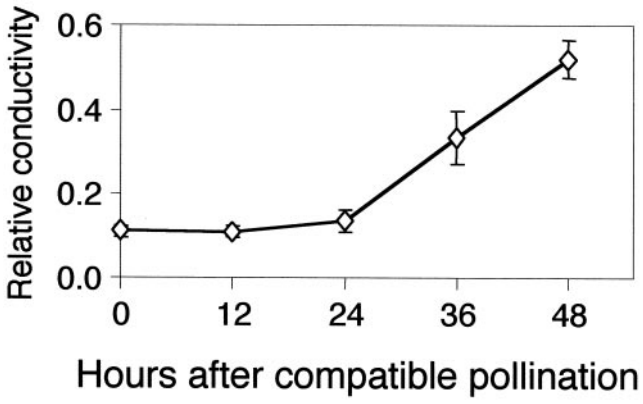


**Figure 3.** Relative conductivity profile after compatible pollination. Each time point represents 56 corollas, with eight corollas taken for each time point during seven different experiments. Relative conductivity is the ratio of sample conductivity to total conductivity (see "Materials and Methods"). SD is indicated as error bars on the average data.

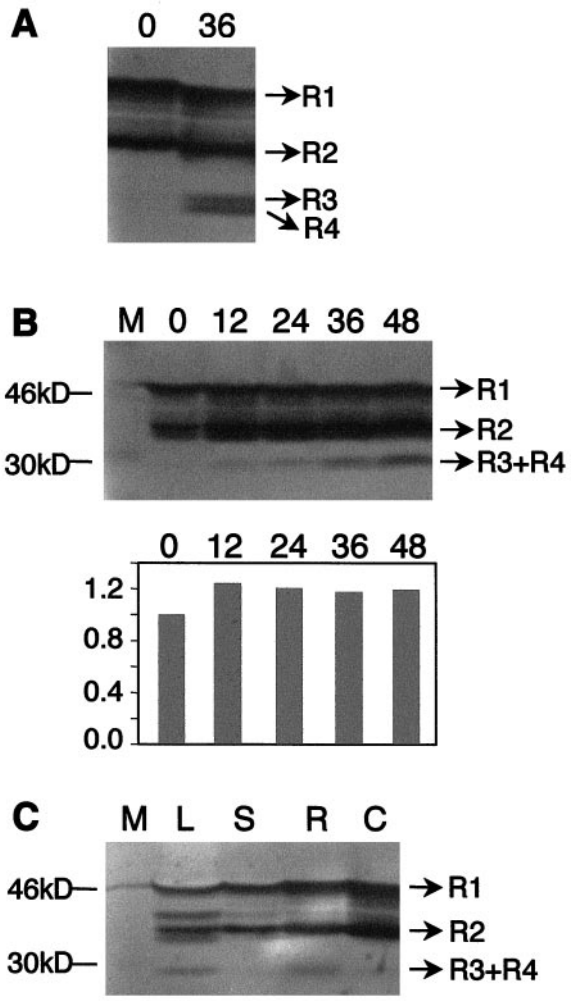


**Figure 4.** Characterization of RNase activities during petal senescence. Fifty micrograms of total corolla protein from different time points was used for RNase detection. Petunia total RNA was incorporated into the resolving gel at 40 $\mu$g/mL. A, Detection of RNase activities in open corollas and corollas at 36 HACP on 12% SDS-PAGE. B, Time course induction of RNases separated on 10% SDS-PAGE after compatible pollination over the senescing period (top). The bottom bar graph shows densitometry data of the total activity of R1 and R2 relative to the activity in open flowers. C, Tissue-specific expression of RNases on a 10% SDS-PAGE gel. M, Rainbow marker; L, young leaf; S, young stem; R, root; C, corolla from open flowers; 0, 12, 24, 36, and 48, HACP.

These results suggest that the initial RNA degradation is partially due to the increased activity of constitutive RNases.

To investigate whether the two constitutive RNases were petal specific, 50 $\mu$g of total protein extracts from other tissues (leaf, stem, and root) was subjected to an in-gel RNase activity assay. Figure 4C shows that the activities of both R1 and R2 were present in all of the tissues tested, suggesting that R1 and R2 are not petal specific but, rather, are involved in non-specific degradation of foreign RNAs or endogenous RNAs. In contrast, R3 and R4 are developmentally regulated.

### Cyt *c* Is Not Released during Petal Senescence

During apoptosis in animal systems, the release of Cyt *c* occurs before visible morphological changes. To investigate Cyt *c* relocation during PIPS, corolla tissues from 0, 24, and 30 HACP were fractionated to separate the cytosol and mitochondria by differential centrifugation. Preliminary experiments showed that plant Cyt *c* reacts with a monoclonal anti-Cyt *c* antibody from Pharmingen but not with one from Calbiochem.

Figure 5 shows that Cyt *c* was detected in crude corolla extract (A, lanes 1 and 6), the supernatant devoid of nuclei and chloroplasts (S, lanes 2, 7, and 11), mitochondrial extracts (M, lanes 4, 9, and 13), and the pellet containing nuclei and chloroplasts (P, lanes 5, 10, and 14). This distribution of Cyt *c* signal is consistent with the location of Cyt *c* in mitochondria and thylakoids (Kranz et al., 1998). In contrast to the accumulation of Cyt *c* in the cytosol during animal apoptosis (Yang et al., 1997), no Cyt *c* was detected in the cytosol at 24 HACP, and only trace amounts of Cyt *c* were detected at 0 and 30 HACP, possibly due to sample leakage from neighboring wells during electrophoresis. To confirm this, fractions of cytosol and mitochondria at 0, 24, and 30 HACP were reloaded, separated, and subjected to immunoblotting with the same antibody. Cyt *c* was consistently detected in mitochondria at equal levels, but absent from the cytosol at all time points (Fig. 6). Considering that the petals had collapsed at 30 HACP (data not shown), our results suggest that the release of Cyt *c* is not involved in early signaling cascade during PIPS, which is in marked contrast to the critical role of Cyt *c* release in apoptosis in animal systems.

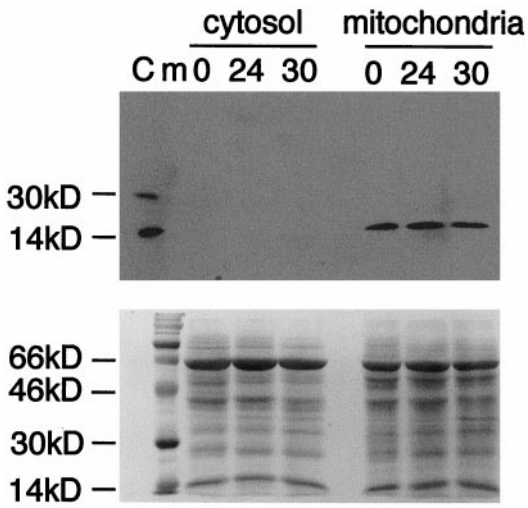


**Figure 6.** Distribution of Cyt *c* during pollination-induced petal senescence. Immunoblot of a 12% SDS-PAGE gel probed with a monoclonal anti-Cyt *c* antibody (top). The bottom panel shows Ponceau staining of the same gel as a loading control. Bovine Cyt *c* (40 ng, lane C) was used as a positive control (15 kD). m, Rainbow marker; 0, 24, and 30, HACP.

### DNA Laddering Coincides with Wilting Symptoms

DNA laddering is one hallmark feature of the late stages of PCD. To visualize DNA ladder formation in senescing petals, *P. inflata* genomic DNA extracts from 0, 12, 24, and 36 HACP were separated, transferred to nylon membranes, and hybridized with radiolabeled *Petunia* genomic DNA. The typical DNA ladder with an increment of 160 bp appears at 36 HACP (Fig. 7A), which is also present in the natural wilting process 6 d after flower opening (Fig. 7B).

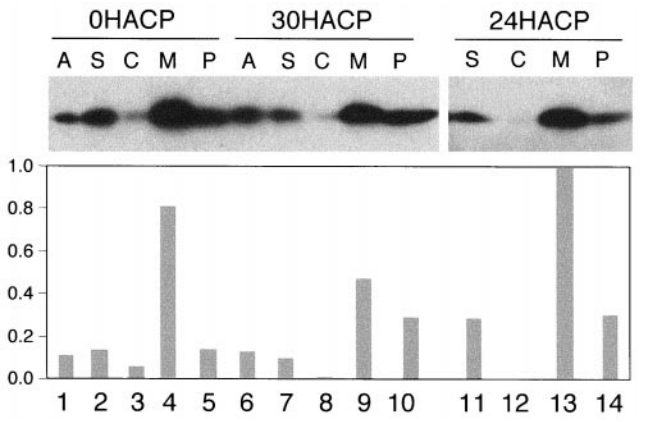


**Figure 5.** Abundance of Cyt *c* in cellular fractions at flower opening and following compatible pollination. Immunoblot of a 12% SDS-PAGE gel was probed with a monoclonal anti-Cyt *c* antibody. A, Crude petal extract; S, 1,500*g* supernatant (extract devoid of nuclei and chloroplasts); C, 16,000*g* supernatant (cytosol); M, 16,000*g* pellet (mitochondria); and P, 1,500*g* pellet (nucleus and chloroplast). Bar graph indicates comparative densitometry data of the Cyt *c* signal with the highest signal in mitochondria as 1.

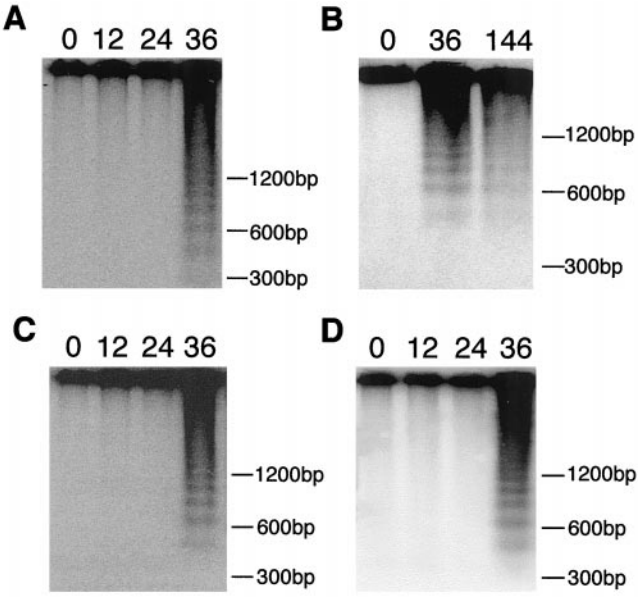


**Figure 7.** Analysis of *P. inflata* for DNA fragmentation. Equal amounts of genomic DNA (2 $\mu$g for A–C; 8 $\mu$g for D) were separated on a 2% (w/v) agarose gel and then transferred to a nylon membrane. The membrane was probed with *Sau*3A1-digested *P. inflata* genomic DNA (A and B), a *Petunia* repetitive DNA (C), and *Brassica* 25S rDNA (D). 0, 12, 24, and 36, HACP; 144, hours after flower opening.

To explore whether the DNA degradation associated with wilting symptoms is sequence specific, several probes were used to detect potential differences in the DNA ladder pattern and band strength. When a repetitive DNA sequence or a 25S rDNA fragment was used as the probe for hybridization, the same DNA ladders with an increment of 160 bp were obtained (Fig. 7, C and D). In addition, hybridization with two senescence-related, low-copy number genes resulted in the detection of only the top intact genomic DNA (data not shown), implying that there are no favorable digestion sites around these genes. Therefore, the DNA degradation is likely to be random.

### Multiple Deoxyribonucleases Are Activated in Senescing Petals

DNA degradation could be mediated by DNases with either single-strand (ss) or double-strand (ds) specific activities. To investigate whether the DNA degradation associated with wilting is due to ssDNase activities or dsDNase activities, an in-gel DNase activity assay was performed. The conditions were optimized for detection of the maximum number of DNase activities. Fifty micrograms of total protein extracts purified from senescing corollas at different time points was separated on 10% polyacrylamide gels containing either ssDNA or dsDNA from salmon sperm, and subjected to treatments to reveal DNase bands, as described in "Materials and Methods."

In the presence of ssDNA, five DNase bands (D1, D2, D3, D4, and D5) were observed (Fig. 8A). Activities of all ssDNase bands increased during senescence (Figs. 8A and 9). In the presence of dsDNA, four DNase bands, corresponding to D2, D3, D4, and D5 in Figure 8A, were observed that increased during senescence (Fig. 8B). The band corresponding to D1 was absent on the dsDNase activity gel, suggesting that this band may be ssDNA specific. Since both ssDNase and dsDNase activities increased over time during PIPS, it is likely that genomic DNA degradation resulted from the activation of both types of DNase activities.

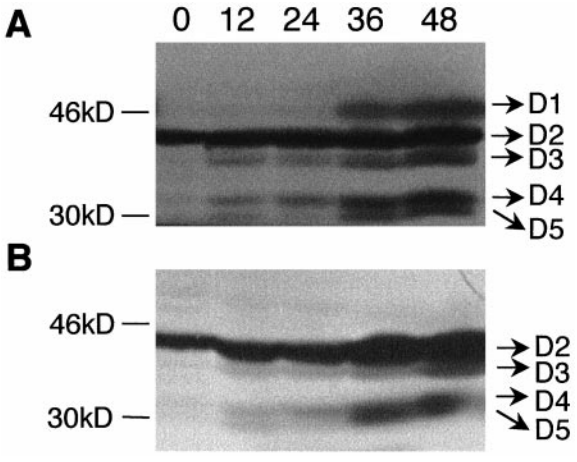


**Figure 8.** Characterization of ssDNase and dsDNase activities during petal senescence. Fifty micrograms of total corolla protein from different time points was separated on a 10% (w/v) SDS-PAGE gel for ssDNase (A) and dsDNase (B) detection. Salmon DNA was used as the substrate. 0, 12, 24, 36, and 48, Hours after compatible pollination.

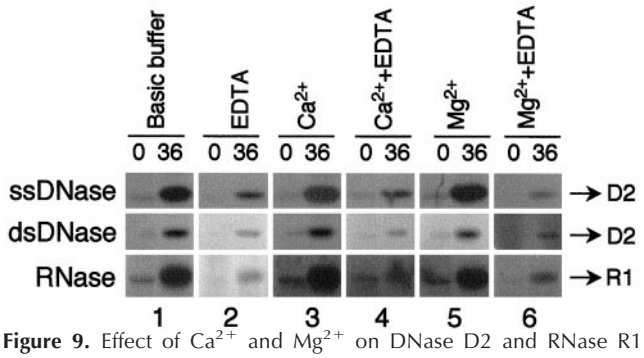


**Figure 9.** Effect of $Ca^{2+}$ and $Mg^{2+}$ on DNase D2 and RNase R1 activities in corolla tissue at 0 and 36 HACP. Ten micrograms of total corolla protein at 36 HACP was separated on 10% SDS-PAGE gels for detection of ssDNase (D2), dsDNase (D2), and RNase (R1). After renaturation, the protein gel was incubated in basic buffer or basic buffer plus one of the following: 1 mM EDTA, 1 mM $CaCl_2$, 1 mM $CaCl_2$ plus 1 mM EDTA, 1 mM $MgCl_2$, and 1 mM $MgCl_2$ plus 1 mM EDTA.

### Bivalent Ions Promote Both DNase Activity and RNase Activity

Since $Ca^{2+}$ has been shown to enhance DNase activities in animal apoptosis, the effects of bivalent ions on RNase and DNase activities were tested. Because preliminary results showed that all five DNase activities and four RNase activities were enhanced by either $Ca^{2+}$ or $Mg^{2+}$ (data not shown), all activity tests were done in the presence of $Ca^{2+}$ (20 $\mu$M) and $Mg^{2+}$ (10 $\mu$M) in the basic buffer. As visible in Figures 4B and 8, the use of high protein amounts (50 $\mu$g) led to saturation of some of the enzymatic activities. To determine whether the major nucleases also increase over time, 10 $\mu$g of total protein was separated on SDS-PAGE gels, renatured in renaturation buffer B, and examined for activities of major DNase D2 and major RNase R1. As shown in Figure 9, both DNase and RNase had higher levels of activity in wilted petals at 36 HACP than at 0 HACP. Both DNase and RNase activities were inhibited by EDTA, a chelator for $Ca^{2+}$ and $Mg^{2+}$ (compare lanes 1 and 2). The addition of higher concentrations of $Ca^{2+}$ or $Mg^{2+}$ (1 mM) in the reaction buffer did not enhance the activity much further (compare lanes 1, 3, and 5), suggesting that the amount of bivalent ions in the basic buffer was at a saturation level. Complete chelation of bivalent ions by including 1 mM EDTA in the reaction buffer reduced DNase activities and RNase activity to similar levels (compare lanes 2, 4, and 6).

## DISCUSSION

We have investigated a number of aspects of PIPS in *P. inflata*. Our results are consistent with the current knowledge that petal senescence is associated with water loss, a decrease in RNA and protein content, and an increase in membrane leakage. The degradation of total RNA is likely caused by both constitutive RNases and induced RNases.

We also explored the similarity between PIPS and apoptosis in animal cells using two hallmark events in animal apoptosis. One early regulatory event, the accumulation of Cyt *c* in the cytosol, was not detected until the late stage of PIPS, when the flower had collapsed. The other most widely used criterion for apoptosis, DNA laddering, was present in wilted petals. We also showed that both RNases and DNases can be activated by bivalent ions.

Successful compatible pollination orchestrates cooperative developmental pathways in different floral organs including accelerated petal senescence (Reid and Wu, 1992). Our observation that only compatible pollination in planta considerably shortens the flower lifespan confirmed the results obtained from detached *P. inflata* flowers (Singh et al., 1992). In addition, compatible pollination in planta also switched the order of two major wilting symptoms, placing floral collapse ahead of petal color change. This implies that different signaling cascades are involved in petal senescence, and can be differentially regulated.

Comparing the time courses of different parameters over the senescence period provided a better understanding of PIPS. Up to 24 HACP, the increase of fresh/dry weight (Fig. 2A) and physical size (Fig. 1) was accompanied by a decrease in RNA (Fig. 2B) and protein amounts (Fig. 2C). Meanwhile, membrane integrity had changed very little (Fig. 3). At this point petal cells were quite intact in terms of membrane integrity, the ability to synthesize new molecules for floral expansion, and the rapid degradation of RNA and protein. At 36 HACP, the wilting symptoms were associated with a decrease in water content or an increase in the ratio of dry weight to fresh weight (Fig. 2A), a continuous decrease in RNA and protein content (Fig. 2, B and C), malfunction of cellular membranes (Fig. 3), and an increase in nuclease activities (Figs. 4 and 8). Taking into account the dramatic differences between 24 and 36 HACP in morphology (Fig. 1), water and weight losses (Fig. 2A, confidence level 95%), membrane leakage (Fig. 3), enzyme activity (Figs. 4 and 8), and DNA laddering (Fig. 7), the massive disassembly stage seems to be between 24 and 36 HACP. This timing coincides with the peak production of ethylene in petal tissues 24 HACP (Singh et al., 1992).

An increase in RNase activity has been associated with a variety of processes, including senescence (Wilson, 1982). The role of RNase in senescence was thought to remobilize phosphate (Wilson, 1982; Taylor et al., 1993). Three major RNases have been shown to increase in senescing petals of daylily, an ethylene-insensitive flower (Panavas et al., 1998b). Our RNase activity assay showed that several RNase activities also increase in senescing corollas of *P. inflata*, an ethylene-sensitive flower. Two major constitutive RNase activities (R1 and R2) were present in all the healthy tissues tested (Fig. 4C), suggesting their wide involvement in RNA degradation. During PIPS, the up-regulation of constitutive R1 and R2 activities was accompanied by the activation of two new RNase bands (R3 and R4) (Fig. 4, A and B). The continuous decrease in RNA amount after pollination (Fig. 2A) and the relatively low activities of R3 and R4 until 24 HACP (Fig. 4B) suggests that PIPS mobilizes both constitutive RNases and new RNases in RNA degradation. However, it does not rule out the possibility that certain RNAs are selectively degraded during senescence.

DNA laddering is widely present in plant PCD, including natural petal senescence in pea (Orzaez et al., 1997b). We were able to detect the presence of a typical DNA ladder with an increment of 160 bp in corolla tissues at 36 HACP during PIPS (Fig. 7A) and naturally occurring senescence 6 d after flower opening in *P. inflata* (Fig. 7B). These results indicate that DNA ladder formation is a common feature associated with petal senescence. To investigate whether this DNA laddering is sequence specific, we determined whether differences in DNA ladder pattern or banding strength could be detected using different probes. Four different probes were tested, including two probes present at a high copy number in the genome and two senescence-related genes with a low copy number. Hybridization with a *Petunia* repetitive DNA (Fig. 7C) or a *Brassica* 25S rDNA (Fig. 7D) revealed the same DNA ladder as probing with genomic DNA (Fig. 7A). When two low-copy-number genes that are up-regulated during petal senescence (data not shown) were used for hybridization, only the top undigested DNA was detected. These results suggest that there are no favorable digestion sites surrounding these four sequences. The failure to detect small DNA banding by the two senescence-related genes may be due to the weak signal caused by the low copy number of the probes. Our data are consistent with non-specific cleavage at internucleosomal points that leads to the formation of a ladder of 160-bp multiples.

Consistent with the detection of both ssDNA and dsDNA cleavage in apoptosis (Bortner et al., 1995), one deoxyribonuclease purified from nuclei undergoing the hypersensitive response showed activity toward both ssDNase and dsDNA (Mittler and Lam, 1995). Our in-gel DNase activity assay showed that both ssDNase and dsDNase activities were induced in senescing corollas (Fig. 8), implying that the cleavage of genomic DNA may happen at both ssDNA and dsDNA sites. In contrast to the induction of new DNase activities at 12 HACP (Fig. 8), the DNA ladder was not detectable until 36 HACP (Fig. 7). This could be explained by a change in the accessibility of genomic DNA to DNases. Both different compartmentation of DNases and genomic DNA and the integrity of chromosomal structure may protect DNA from degradation at the early stages of PIPS. At 36 HACP, leaky membranes and the disintegration of chromosomal structures may expose genomic DNA for degradation.

A large number of studies have shown consistently that apoptosis is associated with an elevated level of intracellular $Ca^{2+}$ (Nicotera and Rossi, 1994; McConkey and Orrenius, 1997). In plants, elevation of $Ca^{2+}$ has also been involved in cell death processes, including hypersensitive response cell death, tracheary cell death, aleurone cell death, leaf senescence, and petal senescence (Leshem, 1987; Porat et al., 1995; Levine et al., 1996; Kuo et al., 1996; Xu and Heath, 1998; Groover and Jones, 1999). The application of $Ca^{2+}$ increases both DNase activity and DNA laddering in both animal cells and plant cells (Bortner et al., 1995; Wang et al., 1996a). Our results are consistent with the published results in that both DNase and RNase activities

were activated by $Ca^{2+}/Mg^{2+}$ and inhibited by EDTA (Fig. 9).

Cyt *c* is an electron transport protein involved in respiration and photosynthesis (Kranz et al., 1998). In apoptosis, release of Cyt *c* from the mitochondrial intermembrane space into the cytosol precedes any morphological changes (Bossy et al., 1998). The translocation of Cyt *c* into the cytosol was detected in maize cell suspensions after D-Man treatment (Stein and Hansen, 1999). However, the timing of this Cyt *c* release was correlated with the onset of DNA laddering, which is characteristic of the late execution stage of cell death processes. In *P. inflata* PIPS, Cyt *c* remained localized in organelles until the flower shape has collapsed (30 HACP) (Fig. 6). The discrepancy between PIPS and maize suspension cell death could be due to differences in the experimental systems and death elicitors used. The involvement of Cyt *c* in other types of plant cell death would be informative with regard to the significance and universality of this event.

The retention of Cyt *c* during early PIPS suggests that there are several unique features to this cell death process. First, it is believed that changes in mitochondrial membranes lead to the release of Cyt *c* in apoptosis (Green and Kroemer, 1998). In PIPS it appears that mitochondrial membranes are intact until an advanced stage of cell degeneration. This is in agreement with the observation that the loss of mitochondrial and nuclear membrane integrity occurs late in leaf senescence (Smart, 1994). Since plant Cyt *c* is located in both mitochondria and plastids (Kranz et al., 1998), the absence of cytosolic Cyt *c* (Figs. 5 and 6) is evidence of the integrity of the mitochondrial and plastid membranes until late in PIPS. Second, cytosolic Cyt *c* is unlikely to be involved in the early signaling network from compatible pollination until floral collapse in *P. inflata.* This is in contrast to apoptosis in animal systems, in which the released Cyt *c* functions as an early regulatory molecule to activate downstream caspases. Although Cys proteases have been reported to be involved in petal senescence (Jones et al., 1995), the mechanism of Cys protease activation in PIPS is likely to be different from that of animal caspases.

It is possible that the PCD mechanisms in plants and animals have their own unique features as a consequence of the fundamental differences in cellular organization, life cycles, developmental patterns, and response to the environment (Mittler, 1998). First, animal PCD aims to eliminate the dying cells completely without causing any side effects. Plants are much more tolerant of aberrant cell death or overgrowth as an organism and the remains of dead plant cells are even required for proper plant functioning, such as in tracheary development (Fukuda, 1997). The release of cellular debris into the intercellular space can cause an inflammatory response in animals, while such an immune reaction is absent from plant cells. Second, plant cells are immobile, restricted by rigid cell walls, which prevents the recycling of the cellular content of dead cells via engulfment of apoptotic bodies. Therefore, contents of dying plant cells may be degraded to small molecules and transported to other cells (Mittler, 1998). Third, a plant cell has two unique organelles, the chloroplast and the vacuole, which may give unique features to plant cell death. Fourth, the cell fate of a plant cell is much less determined than that of an animal cell; therefore, even when important cells die, their neighboring cells can differentiate or redifferentiate to take over their function, while in animal cells, some types of dead cells cannot be replaced.

Evidence for mechanisms unique to plant PCD are accumulating. First, plant homologs of regulatory molecules important to apoptosis in animals have not been identified or shown to be related to plant cell death. Members of the Bcl-2 family and mitochondria play critical roles in apoptosis (Reed, 1997a, 1997b); however, the sequence of a Bcl-2 homolog has not yet been reported in plants, despite recent increases in plant gene sequences from genomics projects. In addition, the expression of Bcl-$x_L$ could not inhibit pathogen-induced cell death in tobacco (Mittler et al., 1996). Though there are plant homologs to DAD-1, which specifies an anti-apoptotic activity in animals, the function of DAD-1 in plants is unknown (Gallois et al., 1997; Tanaka et al., 1997). Second, changes in both chloroplasts and vacuoles have been detected in the early stages of plant cell death. Leaf senescence is believed to initiate from signals from the chloroplast (Smart, 1994). During the hypersensitive response of tobacco to tobacco mosaic virus, an increase in monomeric chloroplast DNA occurred before gross changes in nuclear morphology and significant chromatin cleavage (Mittler et al., 1997). Vacuolization is a very early event in xylogenesis (Groover and Jones, 1999). Third, although Cys proteases are involved in all types of plant PCD studied so far (Fukuda, 1997; Del and Lam, 1998; Solomon et al., 1999; Xu and Chye, 1999), it is not known whether these Cys proteases are similar to animal caspases in terms of activation and substrates. In *P. inflata* PIPS, Cyt *c* was undetectable in the cytosol at a late stage of senescence (Fig. 6), arguing against the involvement of Cyt *c* in the activation of Cys proteases during the early stage of petal senescence. Last, despite the early changes in mitochondria during apoptosis in animals, the loss of structural integrity of mitochondrial and nuclear membranes occurs at the late stage in leaf senescence (Smart, 1994). Since plant Cyt *c* is located in both mitochondria and plastids (Kranz et al., 1998), the absence of cytosolic Cyt *c* (Figs. 5 and 6) is evidence for the intactness of the mitochondrial and plastid membranes until the late stages of PIPS.

## ACKNOWLEDGMENTS

We thank Kristin A. Kolberg for the use of the conductivity meter, Stéphane P. Bentolila for providing the *Petunia* repetitive DNA probe, and June B. Nasrallah for providing the *Brassica* 25S rDNA clone. We are grateful to Rainer H. Köhler and Ikeda Seishi for valuable discussions and technical help.

Received September 1, 1999; accepted December 21, 1999.

## LITERATURE CITED

**Blank A, McKeon TA** (1991) Three RNases in senescent and nonsenescent wheat leaves characterization by activity staining in sodium dodecyl sulfate-polyacrylamide gels. Plant Physiol **97:** 1402–1408

**Borochov A, Spiegelstein H, Philosoph HS** (1997) Ethylene and flower petal senescence: interrelationship with membrane lipid catabolism. Physiol Plant **100:** 606–612

**Bortner CD, Oldenburg-Nicklas BE, Cidlowski JA** (1995) The role of DNA fragmentation in apoptosis. Trends Cell Biol **5:** 21–26

**Bossy WE, Newmeyer DD, Green DR** (1998) Mitochondrial cytochrome *c* release in apoptosis occurs upstream of DEVD-specific caspase activation and independently of mitochondrial transmembrane depolarization. EMBO J **17:** 37–49

**Cai J, Yang J, Jones DP** (1998) Mitochondrial control of apoptosis: the role of cytochrome *c*. Biochim Biophys Acta **1366:** 139–149

**Callard D, Axelos M, Mazzolini L** (1996) Novel molecular markers for late phases of the growth cycle of *Arabidopsis thaliana* cell suspension cultures are expressed during organ senescence. Plant Physiol **112:** 705–715

**Clark DG, Richards C, Hilioti Z, Lind IS, Brown K** (1997) Effect of pollination on accumulation of ACC synthase and ACC oxidase transcripts, ethylene production and flower petal abscission in geranium (*Pelargonium* × *hortorum* L.H. Bailey). Plant Mol Biol **34:** 855–865

**Danon A, Gallois P** (1998) UV-C radiation induces apoptotic-like changes in *Arabidopsis thaliana*. FEBS Lett **437:** 131–136

**Del PO, Lam E** (1998) Caspases and programmed cell death in the hypersensitive response of plants to pathogens. Curr Biol **8:** 1129–1132

**Do YY, Huang PL** (1997) Characterization of a pollination-related cDNA from *Phalaenopsis* encoding a protein which is homologous to human peroxisomal acyl-CoA oxidase. Arch Biochem Biophys **344:** 295–300

**Ellis RE, Yuan J, Palade GE, Horvitz HR** (1991) Mechanisms and functions of cell death. Annu Rev Cell Biol **7:** 663–698

**Finucane DM, Bossy WE, Waterhouse NJ, Cotter TG, Green DR** (1999) Bax-induced caspase activation and apoptosis via cytochrome *c* release from mitochondria is inhibitable by Bcl-$x_L$. J Biol Chem **274:** 2225–2233

**Fukuda H** (1997) Tracheary element differentiation. Plant Cell **9:** 1147–1156

**Fulton TM, Chunwongse J, Tanksley SD** (1995) Microprep protocol for extraction of DNA from tomato and other herbaceous plants. Plant Mol Biol Rep **13:** 207–209

**Gallois P, Makishima T, Hecht V, Despres B, Laudie M, Nishimoto T, Cooke R** (1997) An *Arabidopsis thaliana* cDNA complementing a hamster apoptosis suppressor mutant. Plant J **11:** 325–331

**Green DR** (1998) Apoptotic pathways: the roads to ruin. Cell **94:** 695–698

**Green DR, Kroemer G** (1998) The central executioners of apoptosis: caspases or mitochondria? Trends Cell Biol **8:** 267–271

**Green DR, Reed JC** (1998) Mitochondria and apoptosis. Science **281:** 1309–1311

**Greenberg JT** (1996) Programmed cell death: a way of life for plants. Proc Natl Acad Sci USA **93:** 12094–12097

**Groover A, Jones AM** (1999) Tracheary element differentiation uses a novel mechanism coordinating programmed cell death and secondary cell wall synthesis. Plant Physiol **119:** 375–384

**Hoekstra FA, Weges R** (1986) Lack of control by early pistillate ethylene of the accelerated wilting of *Petunia hybrida* flowers. Plant Physiol **80:** 403–408

**Jacobson MD, Weil M, Raff MC** (1997) Programmed cell death in animal development. Cell **88:** 347–354

**Jiang WB, Mayak S, Weiss D, Halevy AH** (1994) Regulation of a petal-specific ethylene-induced 70-KDa protein from *Dianthus caryophyllus*. Physiol Plant **92:** 219–226

**Jones AM, Dangl JL** (1996) Logjam at the Styx: programmed cell death in plants. Trends Plant Sci **1:** 114–119

**Jones ML, Larsen PB, Woodson WR** (1995) Ethylene-regulated expression of a carnation cysteine proteinase during flower petal senescence. Plant Mol Biol **28:** 505–512

**Jones ML, Woodson WR** (1999) Differential expression of three members of the 1-aminocyclopropane-1-carboxylate synthase gene family in carnation. Plant Physiol **119:** 755–764

**Jones RB, Serek M, Kuo CL, Reid MS** (1994) The effect of protein synthesis inhibition on petal senescence in cut bulb flowers. J Am Soc Hortic Sci **119:** 1243–1247

**Katsuhara M** (1997) Apoptosis-like cell death in barley roots under salt stress. Plant Cell Physiol **38:** 1091–1093

**Katsuhara M, Kawasaki T** (1996) Salt stress induced nuclear and DNA degradation in meristematic cells of barley roots. Plant Cell Physiol **37:** 169–173

**Koukalova B, Kovarik A, Fajkus J, Siroky J** (1997) Chromatin fragmentation associated with apoptotic changes in tobacco cells exposed to cold stress. FEBS Lett **414:** 289–292

**Kranz R, Lill R, Goldman B, Bonnard G, Merchant S** (1998) Molecular mechanisms of cytochrome *c* biogenesis: three distinct systems. Mol Microbiol **29:** 383–396

**Kuo A, Cappelluti S, Cervantes CM, Rodriguez M, Bush DS** (1996) Okadaic acid, a protein phosphatase inhibitor, blocks calcium changes, gene expression, and cell death induced by gibberellin in wheat aleurone cells. Plant Cell **8:** 259–269

**Larson E, Howlett B, Jagendorf A** (1986) Artificial reductant enhancement of the Lowry method for protein determination. Anal Biochem **155:** 243–248

**Lawton KA, Huang B, Goldsbrough PB, Woodson WR** (1989) Molecular cloning and characterization of senescence-related genes from carnation flower petals. Plant Physiol **90:** 690–696

**Lawton KA, Raghothama KG, Goldsbrough PB, Woodson WR** (1990) Regulation of senescence-related gene expression in carnation flower petals by ethylene. Plant Physiol **93:** 1370–1375

**Lay-Yee M, Stead AD, Reid MS** (1992) Flower senescence in daylily (*Hemerocallis*). Physiol Plant **86:** 308–314

**Leshem YY** (1987) Membrane phospholipid catabolism and calcium ion activity in control of senescence. Physiol Plant **69:** 551–560

**Levine A, Pennell RI, Alvarez ME, Palmer R, Lamb C** (1996) Calcium-mediated apoptosis in a plant hypersensitive disease resistance response. Curr Biol **6:** 427–437

**Mahajan NP, Linder K, Berry G, Gordon GW, Heim R, Herman B** (1998) Bcl-2 and Bax interactions in mitochondrial probed with green fluorescent protein and fluorescence resonance energy transfer. Nat Biotechnol **16:** 547–552

**Maniatis T, Fritsch EF, Sambrook J** (1989) Molecular Cloning: A Laboratory Manual, Ed 2. Cold Spring Harbor Laboratory Press, Cold Spring Harbor, NY

**McConkey DJ, Orrenius S** (1997) The role of calcium in the regulation of apoptosis. Biochem Biophys Res Commun **239:** 357–366

**Meyer RCJ, Goldsbrough PB, Woodson WR** (1991) An ethylene-responsive flower senescence-related gene from carnation encodes a protein homologous to glutathione *S*-transferase. Plant Mol Biol **17:** 277–282

**Mittler R** (1998) Cell death in plants. *In* RA Lockshin, Z Zakeri, JL Tilly, eds, When Cells Die: A Comprehensive Evaluation of Apoptosis and Programmed Cell Death. Wiley-Liss, New York, pp 147–174

**Mittler R, Lam E** (1995) Identification, characterization, and purification of a tobacco endonuclease activity induced upon hypersensitive response cell death. Plant Cell **7:** 1951–1962

**Mittler R, Shulaev V, Seskar M, Lam E** (1996) Inhibition of programmed cell death in tobacco plants during a pathogen-induced hypersensitive response at low oxygen pressure. Plant Cell **8:** 1991–2001

**Mittler R, Simon L, Lam E** (1997) Pathogen-induced programmed cell death in tobacco. J Cell Sci **110:** 1333–1344

**Navarre DA, Wolpert TJ** (1999) Victorin induction of an apoptotic/senescence-like response in oats. Plant Cell **11:** 237–249

**Nicotera P, Rossi AD** (1994) Nuclear $Ca^{2+}$: physiological regulation and role in apoptosis. Mol Cell Biochem **135:** 89–98

**Nooden LD, Guiamet JJ, John I** (1997) Senescence mechanisms. Physiol Plant **101:** 746–753

**Orzaez D, Granell A** (1997a) DNA fragmentation is regulated by ethylene during carpel senescence in *Pisum sativum*. Plant J **11:** 137–144

**Orzaez D, Granell A** (1997b) The plant homologue of the defender against apoptotic death gene is down-regulated during senescence of flower petals. FEBS Lett **404:** 275–278
**Osborne BA, Schwartz LM** (1994) Essential genes that regulate apoptosis. Trends Cell Biol **4:** 394–399
**Panavas T, Reid PD, Rubinstein B** (1998a) Programmed cell death of daylily petals: activities of wall-based enzymes and effects of heat shock. Plant Physiol Biochem **36:** 379–388
**Panavas T, Walker EL, Rubinstein B** (1998b) Possible involvement of abscisic acid in senescence of daylily petals. J Exp Bot **49:** 1987–1997
**Pennell RI, Lamb C** (1997) Programmed cell death in plants. Plant Cell **9:** 1157–1168
**Pontier D, Tronchet M, Rogowsky P, Lam E, Roby D** (1998) Activation of hsr203, a plant gene expressed during incompatible plant-pathogen interactions, is correlated with programmed cell death. Mol Plant-Microbe Interact **11:** 544–554
**Porat R, Halevy AH, Serek M, Borochov A** (1995) An increase in ethylene sensitivity following pollination is the initial event triggering an increase in ethylene production and enhanced senescence of *Phalaenopsis* orchid flowers. Physiol Plant **93:** 778–784
**Raghothama KG, Lawton KA, Goldsbrough PB, Woodson WR** (1991) Characterization of an ethylene-regulated flower senescence-related gene from carnation. Plant Mol Biol **17:** 61–72
**Reed JC** (1997a) Double identity for proteins of the Bcl-2 family. Nature **387:** 773–776
**Reed JC** (1997b) Cytochrome *c*: can't live with it, can't live without it. Cell **91:** 559–562
**Reid MS, Wu MJ** (1992) Ethylene and flower senescence. Plant Growth Regul **11:** 37–43
**Ryerson DE, Heath MC** (1996) Cleavage of nuclear DNA into oligonucleosomal fragments during cell death induced by fungal infection or by abiotic treatments. Plant Cell **8:** 393–402
**Schendel SL, Montal M, Reed JC** (1998) Bcl-2 family proteins as ion-channels. Cell Death Differ **5:** 372–380
**Serek M, Sisler EC, Reid MS** (1995) Effects of 1-MCP on the vase life and ethylene response of cut flowers. Plant Growth Regul **16:** 93–97
**Singh A, Evensen KB, Kao TH** (1992) Ethylene synthesis and floral senescence following compatible and incompatible pollinations in *Petunia inflata*. Plant Physiol **99:** 38–45
**Smart CM** (1994) Tansley review no. 64: gene expression during leaf senescence. New Phytol **126:** 419–448
**Solomon M, Belenghi B, Delledonne M, Menachem E, Levine A** (1999) The involvement of cysteine proteases and protease inhibitor genes in the regulation of programmed cell death in plants. Plant Cell **11:** 431–443
**Stead AD** (1992) Pollination-induced flower senescence. Plant Growth Regul **11:** 13–20
**Stein JC, Hansen G** (1999) Mannose induces an endonuclease responsible for DNA laddering in plant cells. Plant Physiol **121:** 71–79
**Steller H** (1995) Mechanisms and genes of cellular suicide. Science **267:** 1445–1449
**Susin SA, Lorenzo HK, Zamzami N, Marzo I, Brenner C, Larochette N, Prevost MC, Alzari PM, Kroemer G** (1999a) Mitochondrial release of caspase-2 and -9 during the apoptotic process. J Exp Med **189:** 381–393
**Susin SA, Lorenzo HK, Zamzami N, Marzo I, Snow BE, Brothers GM, Mangion J, Jacotot E, Costantini P, Loeffler M, Larochette N, Goodlett DR, Aebersold R, Siderovski DP, Penninger JM, Kroemer G** (1999b) Molecular characterization of mitochondrial apoptosis-inducing factor. Nature **397:** 441–446
**Tanaka Y, Makishima T, Sasabe M, Ichinose Y, Shiraishi T, Nishimoto T, Yamada T** (1997) *Dad-1,* a putative programmed cell death suppressor gene in rice. Plant Cell Physiol **38:** 379–383
**Tang X, Woodson WR** (1996) Temporal and spatial expression of 1-aminocyclopropane-1-carboxylate oxidase mRNA following pollination of immature and mature *Petunia* flowers. Plant Physiol **112:** 503–511
**Taylor CB, Bariola PA, Delcardayre SB, Raines RT, Green PJ** (1993) RNS2: a senescence-associated RNase of *Arabidopsis* that diverged from the S-RNases before speciation. Proc Natl Acad Sci USA **90:** 5118–5122
**Vaux DL, Korsmeyer SJ** (1999) Cell death in development. Cell **96:** 245–254
**Vaux DL, Strasser A** (1996) The molecular biology of apoptosis. Proc Natl Acad Sci USA **93:** 2239–2244
**Wang H, Brandt AS, Woodson WR** (1993) A flower senescence-related mRNA from carnation encodes a novel protein related to enzymes involved in phosphonate biosynthesis. Plant Mol Biol **22:** 719–724
**Wang H, Li J, Bostock RM, Gilchrist DG** (1996a) Apoptosis: a functional paradigm for programmed plant cell death induced by a host-selective phytotoxin and invoked during development. Plant Cell **8:** 375–391
**Wang M, Hoekstra S, van Bergen S, Lamers GEM, Oppedijk BJ, van der Heijden MW, de Priester W, Schilperoort RA** (1999) Apoptosis in developing anthers and the role of ABA in this process during androgenesis in *Hordeum vulgare* L. Plant Mol Biol **39:** 489–501
**Wang M, Oppedijk BJ, Caspers MPM, Lamers GEM, Boot MJ, Geerlings DNG, Bakhuizen B, Meijer AH, van Duijn B** (1998) Spatial and temporal regulation of DNA fragmentation in the aleurone of germinating barley. J Exp Bot **49:** 1293–1301
**Wang M, Oppedijk BJ, Lu X, van Duijn B, Schilperoort RA** (1996b) Apoptosis in barley aleurone during germination and its inhibition by abscisic acid. Plant Mol Biol **32:** 1125–1134
**Wertz IE, Hanley MR** (1996) Diverse molecular provocation of programmed cell death. Trends Biochem Sci **21:** 359–364
**White E** (1996) Life, death, and the pursuit of apoptosis. Genes Dev **10:** 1–15
**Whitehead CS, Halevy AH, Reid MS** (1984) Roles of ethylene and 1-aminocyclopropane-1-carboxylic acid in pollination and wound-induced senescence of *Petunia hybrida*. Physiol Plant **61:** 643–648
**Wilson CM** (1982) Plant nucleases: biochemistry and development of multiple molecular forms. *In* MC Rattazzi, JG Scandalios, GS Whitt, eds, Isozymes: Current Topics in Biological and Medical Research, Vol 6. Alan R. Liss, New York, pp 33–54
**Wilson MR** (1998) Apoptotic signal transduction: emerging pathways. Biochem Cell Biol **76:** 573–582
**Wulster G, Sacalis J, Janes HW** (1982) Senescence in isolated carnation petals: effects of indoleacetic acid and inhibitors of protein synthesis. Plant Physiol **70:** 1039–1043
**Xu FX, Chye ML** (1999) Expression of cysteine proteinase during developmental events associated with programmed cell death in brinjal. Plant J **17:** 321–327
**Xu H, Heath MC** (1998) Role of calcium in signal transduction during the hypersensitive response caused by basidiospore-derived infection of the cowpea rust fungus. Plant Cell **10:** 585–597
**Yang J, Liu X, Bhalla K, Kim CN, Ibrado AM, Cai J, Peng TI, Jones DP, Wang X** (1997) Prevention of apoptosis by Bcl-2: release of cytochrome *c* from mitochondria blocked. Science **275:** 1129–1132
**Yen CH, Yang CH** (1998) Evidence for programmed cell death during leaf senescence in plants. Plant Cell Physiol **39:** 922–927
**Yun Z, Zheng FJ, Ying LS, Zhai ZH** (1999) Apoptosis of mouse liver nuclei induced in the cytosol of carrot cells. FEBS Lett **448:** 197–200
**Zhang XS, O'Neill SD** (1993) Ovary and gametophyte development are coordinately regulated by auxin and ethylene following pollination. Plant Cell **5:** 403–418